Planar Near-Field to Far-Field Transformation Using an Equivalent Magnetic Current Approach

Peter Petre and Tapan K. Sarkar, *Fellow, IEEE*

Abstract—**An alternate method is presented for computing far-field antenna patterns from near-field measurements. The method utilizes near-field data to determine equivalent magnetic current sources over a fictitious planar surface that encompasses the antenna, and these currents are used to ascertain the far fields. Under certain approximations, the currents should produce the correct far fields in all regions in front of the antenna regardless of the geometry over which the near-field measurements are made. An electric field integral equation (EFIE) is developed to relate the near fields to the equivalent magnetic currents. Method of moments (MOM) procedure is used to transform the integral equation into a matrix one. The matrix equation is solved using the conjugate gradient method (CGM), and in the case of a rectangular matrix, a least-squares solution for the currents is found without explicitly computing the normal form of the equation. Near-field to far-field transformation for planar scanning may be efficiently performed under certain conditions by exploiting the block Toeplitz structure of the matrix and using CGM and fast Fourier transform (CGFFT), thereby drastically reducing computation time and storage requirements. Numerical results are presented for several antenna configurations by extrapolating the far fields using synthetic and experimental near-field data.**

I. Introduction

NEAR-FIELD antenna measurements have become widely used in antenna testing since they allow for accurate measurements of antenna patterns in a controlled environment. The earliest works are based on the model expansion method, in which the fields radiated by the test antenna are expanded in terms of planar, cylindrical, or spherical wave functions and the measured near-fields are used to determine the coefficients of the wave functions [1]–[5]. Excellent overviews of the development of near-field scanning techniques are found in papers [6], [7]. The primary drawback of the mode expansion technique is that when a Fourier transform is used, the fields outside the measurement region are assumed to be zero, particularly in the planar and cylindrical case. Consequently the far fields are accurately determined only over a particular angular sector that is dependent on the measurement configuration.

Manuscript received August 5, 1991; revised January 28, 1992.

P. Petre is with Compact Software, 483 McLean Boulevard, Paterson, NJ 07504.

T. K. Sarkar is with the Department of Electrical and Computer Engineering, Syracuse University, Syracuse, NY 13244.

IEEE Log Number 9204902.

Narasimhan and Kumar [8] have recently tried an approach similar to the one presented in this paper, in which measured near fields on a planar surface are used to synthesize source currents of planar arrays or apertures. However, the far fields were not ascertained from the equivalent sources. Furthermore, since the Fourier transform of the near fields was represented in terms of the finite Fourier transform of the measured near fields over a planar surface, all the truncation effects present in the modal expansion method are also found in their technique.

The equivalent current approach that represents an alternate method of computing far fields from measured near fields has been recently explored [9]–[12]. In earlier papers, the radiating antenna is replaced by equivalent electric currents. The idea presented here is to replace the radiating antenna by equivalent magnetic currents that reside on a fictitious surface and encompass the antenna. Under certain approximation these equivalent currents should produce the correct far fields in all regions in front of the antenna.

In this approach the integral equation that pertains to the measured near fields and the equivalent magnetic currents is a decoupled one with respect to the coordinate axes for the planar scanning case. This means that two simple decoupled EFIE's can be formulated, which contain only one component of the measured near fields and currents and can be solved separately, in a parallel fashion.

A method of moments procedure [13] with point matching is used in which the equivalent currents are expanded in terms of two-dimensional pulse basis functions with unknown coefficients. The matrix elements of the resultant matrix equation represent the interaction between the probe and each of the current patches. The matrix may be rectangular or square depending on the number of data points and number of unknown currents chosen. The matrix equation is solved with the CGM [14], and in the case of a rectangular matrix, a least-squares solution is found without explicitly computing the normal form of the equation. Near-field to far-field transformation for planar scanning may be efficiently performed under certain conditions. If the spacing between field points and spacing between currents patches are chosen the same, the resultant matrix is block Toeplitz. The structure of the

0018-926X/92$03.00

matrix can be exploited by noting that a two-dimensional Fourier transform may be utilized to evaluate some terms in CGM. This results in a tremendous decrease in storage and computation. The method has been called CGFFT and has previously been applied to scattering problems [15].

The other feature for our method is that the numerical integration in the process of creating the moment matrix elements can b avoided by taking the limiting case of the integral equation. For this special case, instead of using equivalent magnetic currents as equivalent sources, an equivalent magnetic dipole array is used to replace the aperture of the antenna. If the distance between the source and field points is much larger than the sizes of the current patches, then these patches can be replaced by equivalent Hertzian dipoles. A detailed comparison of the accuracy and limitation of both equivalent currents and equivalent dipole array approximations is given in the present paper.

The theoretical basis for the equivalent current approach is detailed in Section II. The formulation of the EFIE is detailed in Section III. The formulation of the matrix equation using MOM with the application of CGFFT is presented in Section IV. The idea of the equivalent magnetic dipole array approximation is given in Section V. Numerical results for several antenna configurations are presented in Section VI.

II. Theory

Let us consider an arbitrary shaped antenna radiating into free space with the aperture of the antenna being a plane surface, which separates the space into left-half and right-half spaces.

Consider the general equivalent problem as shown in Fig. 1. Because it is postulated that the electromagnetic fields, in the left-half space are zero, a perfect electric conductor can be placed on the plane xy. If it is further assumed as for the general case that the tangential component of the electric field on S_∞ is zero except on S_0 then $\mathbf{M}$ exists only on S_0. Using image theory, the equivalent magnetic current $\mathbf{M}$ can be expressed as

$$\overline{\mathbf{M}} = 2\overline{\mathbf{E}} \times \bar{n} \quad \text{on } S_0 \tag{1}$$

where now $\mathbf{M}$ radiates into free space. We can now use measured near fields to determine $\mathbf{M}$.

It is important to note that in the practical near-field measurement process, usually only the electric near fields are measured. So we are focusing our attention to find the far fields from the measured electric near field only via the equivalent magnetic current approach,

$$\overline{\mathbf{E}}_{\text{meas}} = \overline{\mathbf{E}}(\overline{\mathbf{M}}) \tag{2}$$

where $\mathbf{E}_{\text{meas}}$ is the measured electric near field, and $\mathbf{M}$ is the equivalent magnetic current that exists on S_0. In the remainder of this paper, (2) is solved for the planar scanning cases.

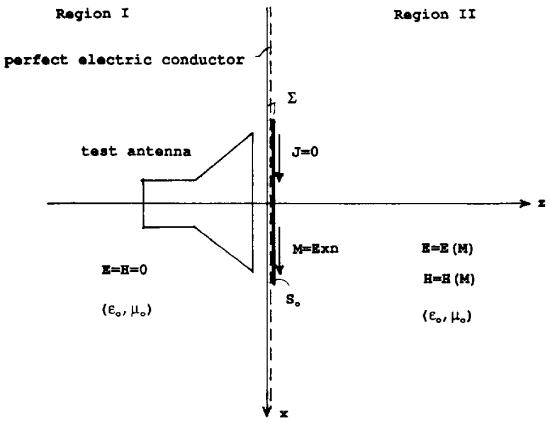

Fig. 1. Equivalent magnetic current approach.

III. Integral Equation Formulation

The electric field at any point P can be found from

$$\overline{\mathbf{E}}(\bar{\mathbf{r}}) = -\int_{S_0}\int [\overline{\mathbf{M}}(\bar{\mathbf{r}}') \times \nabla' g(\bar{\mathbf{r}}, \bar{\mathbf{r}}')]\, ds' \tag{3}$$

where $\mathbf{E}(\mathbf{r})$ is the electric field of an arbitrarily located observation point $\mathbf{r}$, $\mathbf{M}(\mathbf{r}')$ is the equivalent magnetic current at the source point $\mathbf{r}'$, ∇' is the gradient operator according to the primed variables, and $g(\mathbf{r}, \mathbf{r}')$ is the three-dimensional Green's function

$$g(\bar{\mathbf{r}}, \bar{\mathbf{r}}') = \frac{e^{-jk_0|\bar{\mathbf{r}} - \bar{\mathbf{r}}'|}}{4\pi|\bar{\mathbf{r}} - \bar{\mathbf{r}}'|}. \tag{4}$$

Here $k_0 = \omega\sqrt{\mu_0 \epsilon_0}$ is the free-space wave number.

For the planar scanning case, the near-field measurement is performed over a planar surface assumed to be parallel with the source plane as shown in Fig. 2. The aperture of the antenna (S_0) is assumed to be a rectangular plate in the x-y plane with dimension W_x and W_y. The distance between the source plane (S_0) and measurement plane is d. For the planar scanning the x and y components of the electric near fields are usually measured.

Taking only the x and y components of the measured electric near fields into account in (3), the following integral equation can be obtained for the equivalent magnetic currents

$$\begin{bmatrix} E_{\text{meas},x}(\bar{\mathbf{r}}) \\ E_{\text{meas},y}(\bar{\mathbf{r}}) \end{bmatrix} = -\int_{S_0}\int \begin{bmatrix} 0 & \dfrac{\partial g(\bar{\mathbf{r}}, \bar{\mathbf{r}}')}{\partial z'} \\ -\dfrac{\partial g(\bar{\mathbf{r}}, \bar{\mathbf{r}}')}{\partial z'} & 0 \end{bmatrix} \begin{bmatrix} M_x(\bar{\mathbf{r}}') \\ M_y(\bar{\mathbf{r}}') \end{bmatrix} ds'. \tag{5}$$

It is evident from (5) that the obtained integral equation is a decoupled one with respect to the two components of

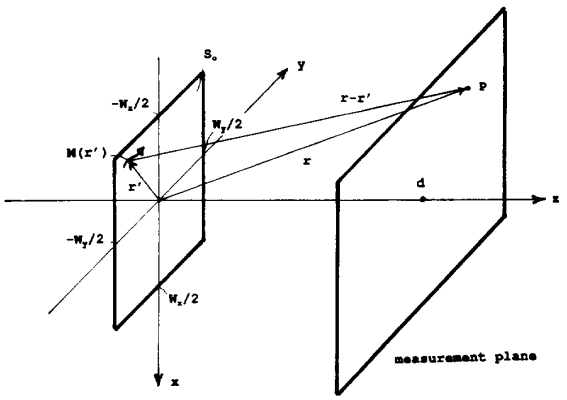

Fig. 2. Planar scanning.

the magnetic currents. So instead of solving (5), the following two simple integral equations can be solved separately:

$$E_{\text{meas},x}(\bar{\mathbf{r}}) = -\int_{S_0}\int \frac{\partial g(\bar{\mathbf{r}},\bar{\mathbf{r}}')}{\partial z'} M_y(\bar{\mathbf{r}}')\, ds' \tag{6a}$$

$$E_{\text{meas},y}(\bar{\mathbf{r}}) = \int_{S_0}\int \frac{\partial g(\bar{\mathbf{r}},\bar{\mathbf{r}}')}{\partial z'} M_x(\bar{\mathbf{r}}')\, ds'. \tag{6b}$$

The present method using the equivalent magnetic current approach is numerically more efficient than the equivalent electric current approach for planar scanning as the integral equation decouples making solutions of large matrix problems quite easy.

IV. Formulation of Matrix Equation

After formulating the E-field integral equations, a MOM procedure is used to transform them into matrix equations. Both components of the equivalent magnetic currents (M_x, M_y) are approximated by equally spaced two-dimensional pulse basis functions

$$M_x(x',y') = \sum_{i=1}^{M}\sum_{j=1}^{N} \boldsymbol{\alpha}_{ij}\Pi_{ij}(x',y') \tag{7a}$$

$$M_y(x',y') = \sum_{i=1}^{M}\sum_{j=1}^{N} \boldsymbol{\beta}_{ij}\Pi_{ij}(x',y') \tag{7b}$$

where $\boldsymbol{\alpha}_{ij}$ and $\boldsymbol{\beta}_{ij}$ are the unknown amplitudes of the x and y directed magnetic currents, respectively on the ijth patch, and $\Pi_{ij}(x',y')$ is the two-dimensional pulse basis function pertaining to the ijth patch and defined as

$$\Pi_{ij}(x',y') = \begin{cases} 1 & \text{if } x_i - \dfrac{\Delta x}{2} \le x' \le x_i + \dfrac{\Delta x}{2} \\ & y_j - \dfrac{\Delta y}{2} \le y' \le y_j + \dfrac{\Delta y}{2}, \\ & \text{and } 0 \quad \text{otherwise.} \end{cases} \tag{8}$$

For the above approximation the aperture plate (S_0) on which the equivalent magnetic currents reside is assumed to be a rectangular one in the x-y plane with extensions $-w_x/2 \le x \le w_x/2$ and $-w_y/2 \le y \le w_y/2$ as shown in Fig. 2. The aperture plate (S_0) is divided into $M \cdot N$ equally spaced rectangular patches with dimensions Δx and Δy

$$\Delta x = w_x/M \tag{9a}$$

$$\Delta y = w_y/N \tag{9b}$$

In (8) x_i and y_j are the x and y coordinates of the center of the ijth patch and are given by

$$x_i = -w_x/2 - \Delta x/2 + i\,\Delta x \tag{10a}$$

$$y_j = -w_y/2 - \Delta y/2 + j\,\Delta y \tag{10b}$$

It is important to note that these simple pulse basis functions can be used to approximate the magnetic currents because the integral equations do not contain any derivatives of these currents. This is a consequence of the previous assumption that the field points and the measurement points, are always outside the current-carrying region (S_0).

Since it is assumed that the measured electric near fields are known at discrete points on the scanning plane a point matching procedure is chosen.

Substituting (7) into (6) and utilizing point matching the following two decoupled matrix equations are obtained,

$$\mathbf{E}_{\text{meas},x} = -\mathbf{G}\mathbf{M}_y \tag{11a}$$

$$\mathbf{E}_{\text{meas},y} = \mathbf{G}\mathbf{M}_x \tag{11b}$$

where $\mathbf{E}_{\text{meas},x}$ and $\mathbf{E}_{\text{meas},y}$ are the vectors that contain the x and y components of the measured electric near fields, respectively, $\mathbf{M}_x$ and $\mathbf{M}_y$ are the vectors that contain the unknown coefficients α_{ij} and β_{ij}, respectively, and, $\mathbf{G}$ is the moment matrix for the planar scanning case. The explicit expressions for matrix $\mathbf{G}$ is given by

$$\mathbf{G}_{k,l} = \int_{\Omega_l}\int \frac{e^{-jk_0R}}{4\pi R^2}(z_k - z')\left[jk_0 + \frac{1}{R}\right] ds' \tag{12}$$

where Ω_1 is the area of the lth patch, and R is the distance between the kth field point $(\mathbf{r}_k)$ and source point $(\mathbf{r}')$.

If the number of measured near-field points are the same as the number of current elements then the solution for (11) is unique. If the number of measured near-field points are larger than the number of current elements a least-squares solution is obtained. Gauss' quadrature formula is used to evaluate the two-dimensional integral numerically in (12), and CGM is used to solve the matrix equations in (11).

The CG method starts with an initial guess $\mathbf{X}_1$ and computes

$$\mathbf{R}_1 = Y_1 - \mathbf{A}\mathbf{X}_1 \tag{13}$$

$$\mathbf{P}_1 = \mathbf{A}^*\mathbf{R}_1 \tag{14}$$

for $i = 1, 2, \cdots$ let

$$a_i = \frac{\|\mathbf{A}^*\mathbf{R}_i\|^2}{\|\mathbf{A}\mathbf{P}_i\|^2} \tag{15}$$

$$\mathbf{X}_{i+1} = \mathbf{X}_i + a_i\mathbf{P}_i \tag{16}$$

$$\mathbf{R}_{i+1} = \mathbf{R}_i - a_i\mathbf{A}\mathbf{P}_i \tag{17}$$

$$b_i = \frac{\|\mathbf{A}^*\mathbf{R}_{i+1}\|^2}{\|\mathbf{A}^*\mathbf{R}_i\|^2} \tag{18}$$

$$\mathbf{P}_{i+1} = \mathbf{A}^*\mathbf{R}_{i+1} + b_i\mathbf{P}_i \tag{19}$$

Here $\mathbf{A}^*$ is the conjugate transpose of $\mathbf{A}$.

Most of the computation in CGM occurs in the calculation of $\mathbf{A}\mathbf{P}_i$ and $\mathbf{A}^*\mathbf{R}_{i+1}$. Exploiting the block Toeplitz structure of the matrix $\mathbf{A}$, the above terms can be computed using a two-dimensional FFT [17],

$$\mathbf{A}\mathbf{P}_i = F^{-1}\{F(\mathbf{A}^c)F(P_i^c)\} \tag{20}$$

$$\mathbf{A}^*\mathbf{R}_{i+1} = f_c F^{-1}\{F(\mathbf{A}^c)F(\mathbf{R}_{i+1}^{c*})\}^* \tag{21}$$

Here F denotes the two-dimensional discrete Fourier Transform, F^{-1} the two-dimensional inverse discrete Fourier Transform, $\mathbf{A}^c$ is the convolution variation of the original matrix $\mathbf{A}$, $\mathbf{P}_i^c$ and $\mathbf{R}_{i+1}$ are the convolution variations of the original vectors $\mathbf{P}_i$, $\mathbf{R}_{i+1}$, respectively, and * denotes conjugate. For an $M \times N$ grid division the matrices $\mathbf{A}^c$, $\mathbf{P}_i^c$ and $\mathbf{R}_{i+1}^c$ are $2M - 1 \times 2N - 1$, and therefore an FFT for nonpowers of two must be utilized to evaluate (20) and (21). A detailed description about the discrete convolution representation of a block Toeplitz system can be found in [17].

Using CGFFT method, for $M \times N$ measured field points, five matrixes of size $2M - 1 \times 2N - 1$ need to be stored, as opposed to one matrix of size $MN \times MN$ and four vectors of size $MN \times 1$ using CGM alone. Furthermore the required computation for the two dimensional FFT's is $(2M - 1)(2N - 1)\log_2(M + N - 1)$ as opposed to $(MN)^2$, using CGM alone.

If the number of measured data points is larger than the number of current elements chosen, a least-squares solution is found without explicitly computing the normal form of the equation. It is important to note that there is no change in the solution procedure when a least-squares formulation is applied.

V. Equivalent Magnetic Dipole Array

Instead of using equivalent magnetic currents as sources in the general magnetic current approach, equivalent magnetic dipole array can also be used to replace the aperture of the test antenna. This approximation can be originated from either a physical or mathematical point of view.

From a mathematical point of view, this equivalent magnetic dipole array approximation can be treated as a limit of the integral equation approach. For this limiting case, it can be assumed that the numerical integrations in the process of creating the moment matrix elements in (12) are executed using a one-point approximation, i.e.,

$$\int_{\Omega_l}\int f(x_k, x', y_k, y')\,ds' \cong \Omega_1 f(x_k, x_1', y_k, y_1') \tag{22}$$

In the above equation Ω_1 is the area of the lth patch, $f(x_k, x', y_k, y')$ is the appropriate function to be integrated, (x_k, y_k, z_k) are the coordinates of the kth field point and (x_1', y_1', z_1') are the coordinates of the center of the lth patch.

If the distance between the source and field points are much larger than the sizes of the current patches,

$$R \gg \max(\Delta X, \Delta y) \tag{23}$$

then the approximation given by equation (22) is valid. In our cases the distance between the source plane and the scanning plane is always much greater than the largest size of the current patch.

Using this one-point approximation in equation (12) an equivalent magnetic dipole array approximation is developed because the right side in equation (22) can be treated as the appropriate electric field component of a magnetic dipole.

From a physical point of view, this equivalent magnetic dipole array approximation can be treated as a special case of the general equivalent current approach.

The advantage of this approximation is that the numerical integration in the process of creating the moment matrix elements can be avoided. This is a very time consuming procedure. The other advantage of using the magnetic dipole array as equivalent sources is that the moment matrix need not be stored in an explicit form. This is because the elements of the moment matrix do not contain numerical integrations. This causes tremendous reduction in the storage requirements and makes the method numerically more efficient.

VI. Numerical Results

Far-field results for several planar antenna configurations are presented in this section. In all examples where planar near fields are used, CGFFT has been employed. In Section VI-A, synthetic near-field data is used to extrapolate the far fields. A comparison is made between the extrapolated and analytic far fields. In Section VI-B, experimental near-field data is utilized to ascertain far fields for a microstrip array. The extrapolated far fields are compared with those obtained using modal expansions.

A. Far Fields Extrapolated from Synthetic Near Fields

In the first example an array of four y-directed electric Hertzian dipoles placed on the corners of a 4λ by 4λ planar surface is considered. A fictitious planar surface in the x-y plane of dimensions 5λ by 5λ is used to form a planar magnetic current sheet. On the surface the equivalent magnetic currents M_x and M_y divided into 25×25 current patches, are assumed. The near fields are sampled on a planar surface of the same dimensions and dis-

cretized to enable use of CGFFT. The distance between the source plane (S_0) and the scanning plane is 3λ. Fig. 3 shows the normalized absolute value of the electric far-field component $|E_\Theta|$ versus Θ in dB for $\Phi = 90$. The analytic solution is also given in the figure. The calculated far fields are accurate up to $\pm 75°$ from $\Theta = 0$. The reason, the difference between the numerical result and the analytic one is larger at the two edges of the characteristic, is that equivalent magnetic currents are used to model pure electric dipoles. The electric and magnetic current elements have different behaviors at $\Theta \simeq \pm 90$. In spite of this, the equivalent magnetic current approach provides acceptable results over the entire elevation range. The conventional planar scanning may not provide accurate results beyond $\tan^{-1}(0.5/3) \approx 10°$ [18].

For the second example, a comparison is made between the results obtained by using the equivalent magnetic current approach and the equivalent magnetic dipole array approximation. Consider an array of four y-directed magnetic dipoles placed on the corners of a 4λ by 4λ planar surface. An equivalent planar surface of size $5\lambda \times 5\lambda$ is chosen and the near fields are sampled over a plane of the same dimensions at a distance of 3λ. The number of current patches for the magnetic current approach and the number of equivalent magnetic dipoles for the magnetic dipole array approximation are 20×20. The number of the measured near-field points are also 20×20. Fig. 4(a) shows the normalized values of $|E_\Phi|$ versus Θ in dB for $\Phi = 90$ with the analytic solution using the magnetic current approach. Fig. 4(b) shows the same normalized far-field component with the analytic solution but using the magnetic dipole array approximation. Both results show excellent agreement with the analytic ones. The difference between the two solutions obtained by using either the magnetic current approach or the magnetic dipole array approximation is negligible.

B. Far Fields Extrapolated from Experimental Data

In this example, far fields obtained using planar measurements and the equivalent magnetic dipole array approximation are compared with those obtained using planar measurements and planar modal expansions. Consider a microstrip array consisting of 32×32 uniformly distributed patches on a 1.5×1.5 m surface. The operating frequency is 3.3 GHz. The array is considered to be in the x-y plane.

For the planar modal expansion approach, the near fields are measured on a plane 3.24×3.24 m at a distance of 35 cm from the array. There are 81×81 points measured 4 cm apart. The 81×81 data points are zero padded to produce 128×128 far-field points. Measurements are performed using a WR 284 waveguide.

For the first equivalent magnetic dipole array approximation, a 1.56×1.56 m surface with 39×39 uniformly distributed magnetic dipoles are used for the source plane and a 3.24×3.24 m surface with 81×81 measured near-field points are used for the field plane. So the solution obtained here is a least-squares one with exploit-

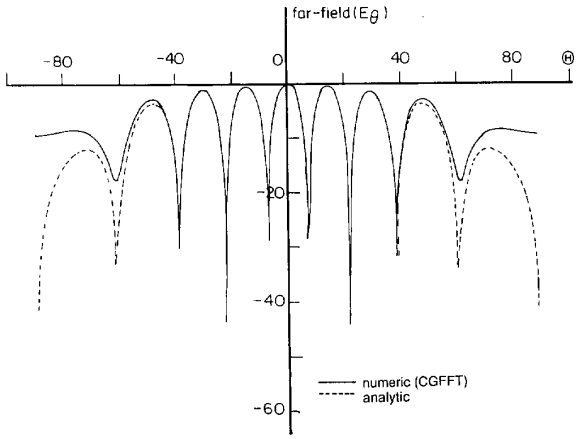

Fig. 3. Comparison of exact and computed far fields for $\Phi = 90$ cut for 2×2 electric dipoles on a $4\lambda \times 4\lambda$ surface using planar scanning.

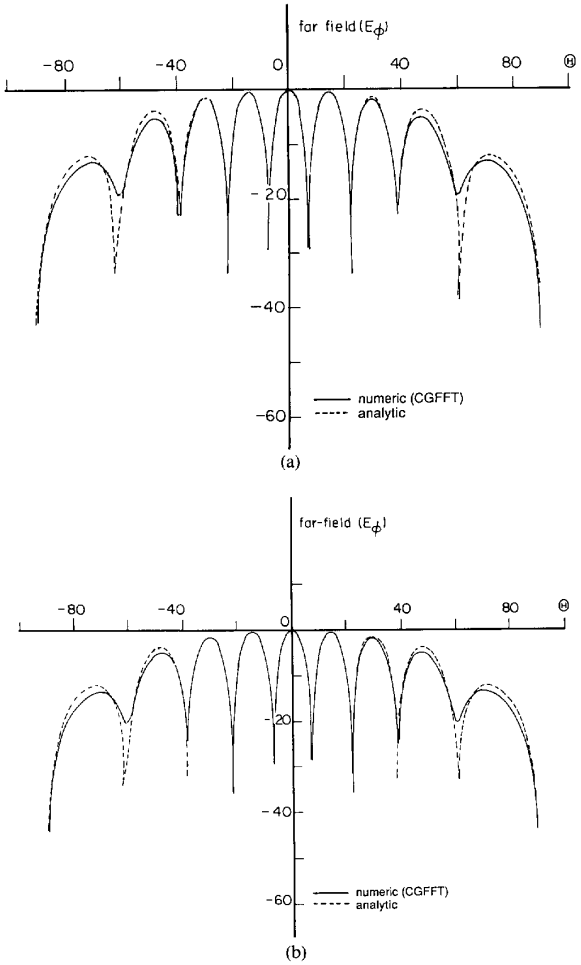

Fig. 4. (a) Comparison of exact and computed far fields for $\Phi = 90$ cut for 2×2 magnetic dipoles on a $4\lambda \times 4\lambda$ surface using planar scanning and equivalent magnetic current approach; (b) comparison of exact and computed far fields for $\Phi = 90$ cut for 2×2 magnetic dipoles on a $4\lambda \times 4\lambda$ surface using planar scanning and equivalent magnetic array approximation.

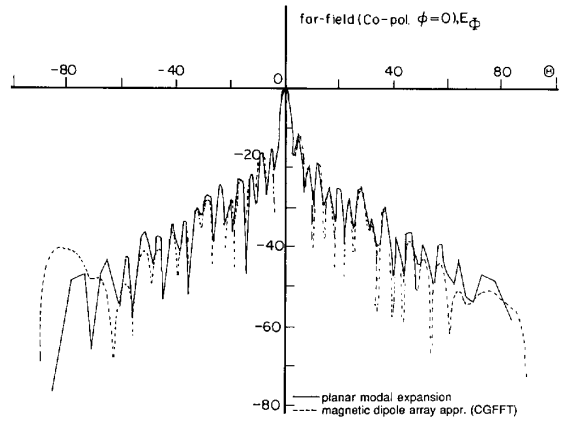

Fig. 5. Copolarization characteristic for $\Phi = 0$ cut for a 32×32 patch microstrip array using planar modal expansion and equivalent magnetic dipole array approximation.

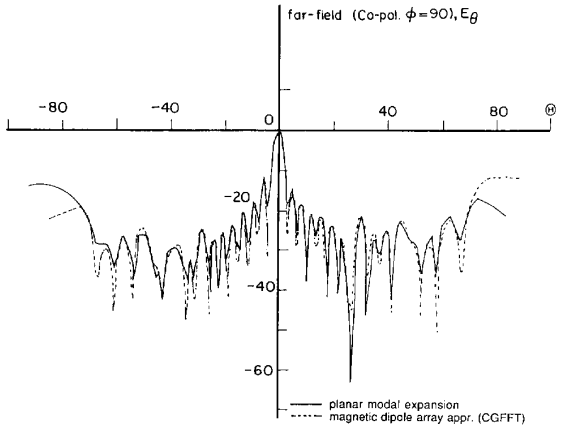

Fig. 6. Copolarization characteristic for $\Phi = 90$ cut for a 32×32 patch microstrip array using planar modal expansion and equivalent magnetic dipole array approximation.

ing the block Toeplitz structure of the matrix and utilizing CGFFT.

Fig. 5 shows the normalized absolute values of the electric far-field component $|E_\Phi|$ versus Θ in dB for $\Phi = 0$ using the equivalent magnetic dipole array approximation and planar modal expansion. This is the copolarization pattern. The result obtained using the equivalent magnetic dipole array approximation and the result obtained using the planar modal expansion show excellent agreement up to $\pm 60°$ of $\Phi = 0°$ and show acceptable agreement in the rest of the elevation range.

Fig. 6 shows the normalized values of $|E_\Theta|$ versus Θ in dB for $\Phi = 90$ using the magnetic dipole array approximation and the planar modal expansion, respectively. The polarization is the main one. The agreement between the results obtained using the different approximations is excellent up to $\pm 60°$ of $\Theta = 0°$ and acceptable in the rest of the elevation range.

Fig. 7 shows the normalized values of $|E_\Theta|$ versus Θ in dB for $\Phi = 0$ using the magnetic dipole array approximation and the planar modal expansion, respectively. This is the cross polarization. The result obtained using the equivalent magnetic dipole array approximation and the result obtained using the planar modal expansion show excellent agreement up to $\pm 60°$ of $\Theta = 0°$ and acceptable agreement in the rest of the elevation range.

Fig. 8 shows the normalized values of $|E_\Phi|$ versus Θ in dB for $\Phi = 90$ using the magnetic dipole array approximation and the planar modal expansion, respectively. This is the cross polarization. The shapes of the curves and the level of the sidelobes are the same for both approximations. Because the level of this cross-polarization characteristics is much lower than the level of the copolarization ones, largest absolute error may be allowed for these curves as for the main polarization characteristics. For Figs. 5–8 it is known that the conventional planar modal expansion would provide acceptable results up to $\tan^{-1}(87/35) = 68°$. Perhaps that is the reason why the

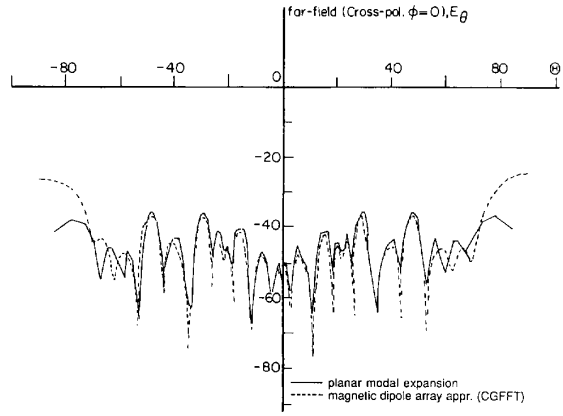

Fig. 7. Cross-polarization characteristic for $\Phi = 0$ cut for a 32×32 patch microstrip array using planar modal expansion and equivalent magnetic dipole array approximation.

planar modal expansion results tend to deviate from our results beyond $\pm 60°$.

For the second equivalent magnetic dipole array approximation, a 1.48×1.48 m surface with 37×37 uniformly distributed magnetic dipoles is used for the source plane, and a 1.48×1.48 m surface with 37×37 measured near-field points is used for the field plane to enable use of CGFFT.

It is important to note that for this case the conventional planar expansion method cannot be used because the area of the measured plane is equal to the area of the actual aperture of the test antenna. So the maximum angle for accurate far field (Θ_s) when the planar modal expansion method is used is equal to zero [18].

Fig. 9 shows the normalized absolute value of the electric far-field component $|E_\Phi|$ versus Θ in dB for $\Phi = 0$ using both equivalent magnetic dipole array approximations. This is the co-polarization pattern. The result obtained using the first approximation and the

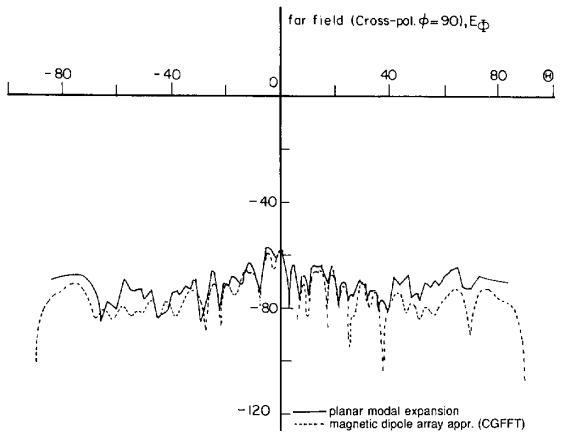

Fig. 8. Cross-polarization characteristic for $\Phi = 90$ cut for a 32×32 patch microstrip array using planar modal expansion and equivalent magnetic dipole array approximation.

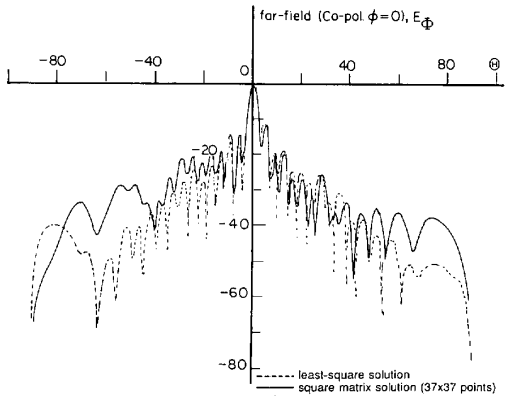

Fig. 9. Copolarization characteristic for $\Phi = 0$ cut for a 32×32 patch microstrip array using least-squares and square matrix solutions.

result obtained using the second one show good agreement up to $\pm 35°$ of $\Theta = 0°$ and show acceptable agreement in the rest of the elevation range. This formulation is more sensitive to the measurement errors than the least squares one.

Fig. 10 shows the normalized values of $|E_\theta|$ versus Θ in dB for $\Phi = 0$ using both equivalent magnetic dipole array approximations. The polarization is the main one. The agreement between the results obtained using the different approximations is excellent up to $\pm 40°$ of $\Theta = 0°$ and acceptable in the rest of the elevation range.

Fig. 11 shows the normalized values of $|E_\theta|$ versus Φ in dB for $\Theta = 0$ using both magnetic dipole array approximations. This is the cross polarization. The result obtained using the first approximation and the result obtained using the second one show good agreement up to $\pm 40°$.

Fig. 12 shows the normalized values of $|E_\Phi|$ versus Θ in dB for $\Phi = 90$ using both magnetic dipole array approximations. This is the cross polarization. The agreement

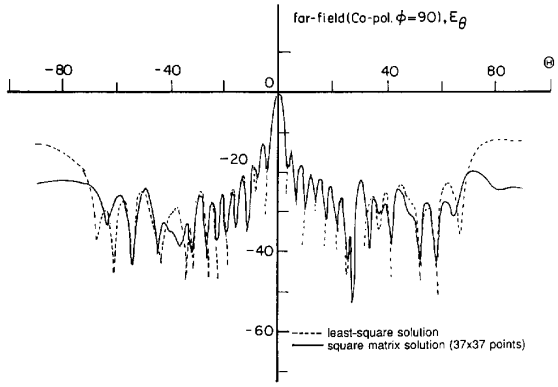

Fig. 10. Copolarization characteristic for $\Phi = 90$ cut for a 32×32 patch microstrip array using least-squares and square matrix solutions.

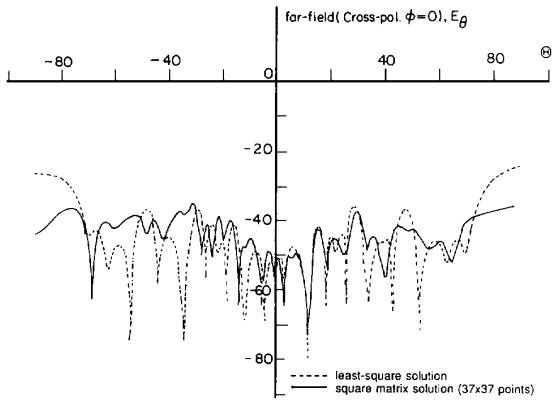

Fig. 11. Cross-polarization characteristic for $\Phi = 0$ cut for a 32×32 patch microstrip array using least-squares and square matrix solutions.

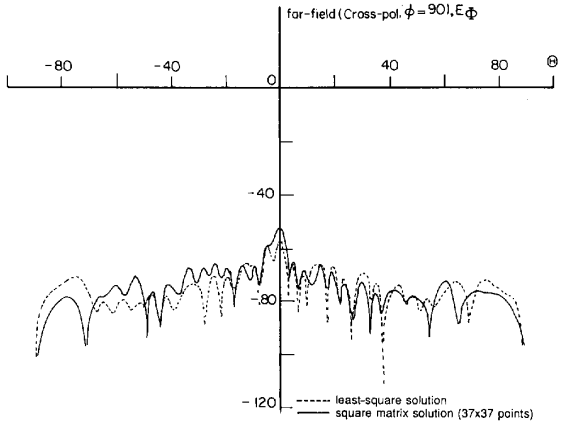

Fig. 12. Cross-polarization characteristic for $\Phi = 90$ cut for a 32×32 patch microstrip array using least-squares and square matrix solutions.

between the results obtained using the different approximations is reasonable in the entire elevation range.

For the final example, we measure the planar near-field data in a narrow region (3.24×0.76 m) and produce the copolar and the crosspolar pattern for $\phi = 0°$ as shown in

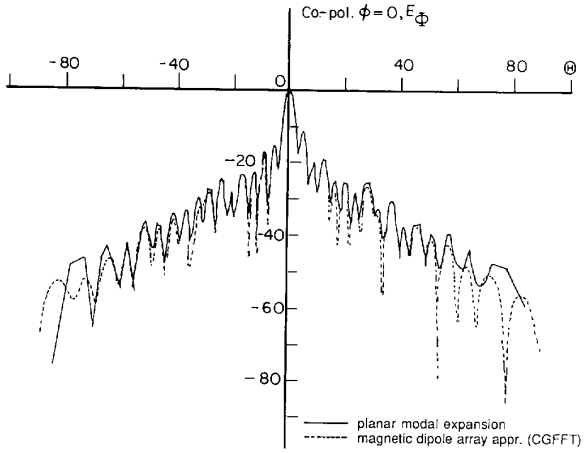

Fig. 13. Copolarization characteristic for $\phi = 0$ cut for the microstrip array when the near-field is measured in a narrow region (3.24 × 0.76 m) as opposed to (3.24 × 3.24 m).

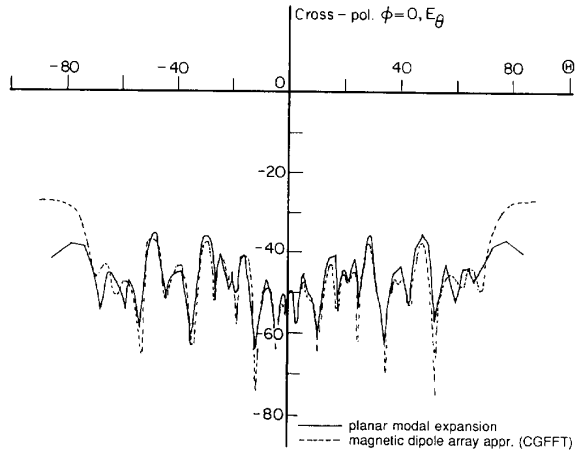

Fig. 14. Cross-polarization characteristic for $\phi = 0°$ for the microstrip array with data measured on a narrow region (3.24 × 0.76 m).

Figs. 13 and 14. The antenna surface is approximated with 39 × 39 uniformly distributed magnetic dipoles on a 1.56 × 1.56 m surface. The number of measurement points are 81 × 19, so a least-squares solution is obtained exploiting the block Toeplitz structure of the matrix and utilizing CGFFT.

It is important to note that the modal expansion method does not allow us to approximate the source and the measurement plates in two different ways. Also in the figures, the results obtained using the modal expansion method are given for comparison.

Similarly, the copolar and the crosspolar patterns of Figs. 15 and 16 for $\phi = 90°$ has been produced from data measured in the narrow region (0.76 × 3.24 m).

Summarizing our experimental results it can be concluded that the equivalent magnetic dipole array approximation gives accurate far-field patterns at angles beyond

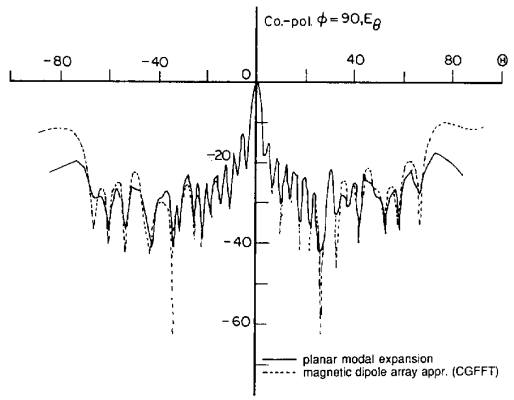

Fig. 15. Copolarization characteristic for $\phi = 90°$ cut for the microstrip array with data measured on a narrow region (0.76 × 3.24 m).

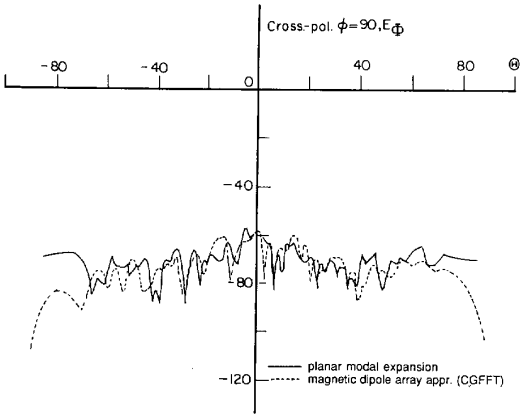

Fig. 16. Cross-polarization characteristic for $\phi = 90°$ cut for the microstrip array with data measured on a narrow region (0.76 × 3.24 m).

which the conventional planar modal expansion technique. For example, for Figs. 9–12, the conventional planar modal expansion will not work [18]. The present approach provides accurate results up to $\pm 40°$ and the deterioration beyond that is graceful. The accuracy of this approximation depends mainly upon the accuracy of the measured near-field data and does not depend on the measurement configuration. When a least-squares solution is obtained for the equivalent sources, the calculated far fields are not so sensitive to the errors in the noisy data as for the approximation when a square matrix solution is done.

IX. Conclusion

A simple method is presented for computing far-field antenna patterns from near-field measurements. The method utilizes near-field data to determine equivalent magnetic source currents or magnetic dipole array over the aperture of the antenna. Using this method it is possible to find the far fields of antennas that are not highly directive over large elevations and azimuthal ranges without using spherical scanning. Furthermore, the far

field may be found with any desired resolution, and interpolation is not required. Under certain conditions CGFFT may be used, thereby drastically reducing computation and storage requirements. Instead of using the equivalent magnetic current approach, a magnetic dipole array approximation is applied, thereby eliminating the numerical integration in the process of creating the moment matrix elements. This method has a wider range of validity than the conventional modal expansion method.

REFERENCES

[1] J. Brown and E. V. Jull, "The prediction of aerial radiation patterns for near-field measurements," in *Proc. Inst. Elec. Eng.*, vol. 108B, pp. 635–644, Nov. 1961.

[2] D. M. Kerns, "Plane-wave scattering-matrix theory of antennas and antenna-antenna interactions," *NBS Monograph 162*, U.S. Govt. Printing Office, Washington, DC, June 1981.

[3] F. Jensen, "Electromagnetic near-field correlations," Ph.D. Dissertation, Tech. Univ. Denmark, July 1970.

[4] W. M. Leach, Jr. and D. T. Paris, "Probe-compensated near-field measurements on cylinder," *IEEE Trans. Antennas Propagat.*, vol. AP-21, pp. 435–445, July 1973.

[5] D. T. Paris, W. M. Leach, E. B. Joy, "Basic theory of probe-compensated near-field measurements," *IEEE Trans. Antennas Propagat.*, vol. AP-26, pp. 373–379, May 1978.

[6] A. D. Yaghjian, "An overview of near-field antenna measurements," *IEEE Trans. Antennas Propagat.*, vol. AP-34, pp. 30–45, Jan. 1986.

[7] J. J. H. Wang, "An examination of the theory and practice of planar near-field measurement," *IEEE Trans. Antennas and Propagat.*, vol. AP-36, pp. 746–753, June 1988.

[8] M. S. Narasimhan and B. P. Kumar, "A technique of synthesizing the excitation currents of planar arrays or apertures," *IEEE Trans. Antennas Propagat.*, vol. AP-38, pp. 1326–1332, Sept. 1990.

[9] T. K. Sarkar, S. Ponnapolli, and E. Arvas, "An accurate efficient method of computing a far-field antenna patterns from near-field measurements," in *Proc. Int. Conf. Antennas Propagat.*, Dallas, TX, May 1990.

[10] S. Ponnapolli, "The computation of far-field antenna patterns from near-field measurements using an equivalent current approach," Ph.D. Dissertation, Syracuse Univ., Dec. 1990.

[11] ——, "Near-field to far-field transformation utilizing the conjugate gradient method," in *Application of conjugate gradient method in electromagnetics and signal processing*, in *PIER*, T. K. Sarkar, ed. New York: VNU Sci. Press, vol. 5, Chapter 11, Dec. 1990.

[12] S. Ponnapolli, T. K. Sarkar, and P. Petre, "Near-field to far-field transformation using an equivalent current approach," in *Proc. Int. Conf. Antennas Propagat.*, London, Ontario, June 1991.

[13] R. F. Harrington, *Field Computation by Moment Methods*. Malabor: Robert E. Kreiger Publishing, 1968.

[14] T. K. Sarkar, E. Arvas: "On a class of finite step iterative methods (conjugate directions) for the solution of an operator equation arising in electromagnetics," *IEEE Trans. Antennas Propagat.*, vol. AP-33, pp. 1058–1066, Oct. 1985.

[15] T. K. Sarkar, E. Arvas, S. M. Rao, "Application of FFT and conjugate gradient method for the solution of electromagnetic radiation from electrically large and small conducting bodies," *IEEE Trans. Antennas Propagat.*, vol. AP-34, pp. 635–640, May 1986.

[16] R. F. Harrington, *Time-Harmonic Electromagnetic Fields*. New York: McGraw-Hill, 1961.

[17] A. V. Oppenheim and R. W. Shafer, *Digital Signal Processing*. Englewood Cliffs, NJ: Prentice-Hall, 1975.

[18] A. C. Newell, "Error analysis techniques for planar near-field measurements," *IEEE Trans. Antennas Propagat.*, vol. AP-36, pp. 754–768, June 1988.

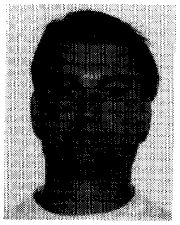

Peter Petre was born in Paszto, Hungary, on February 27, 1961. He received both Dipl. Ing. and Dr. Ing. degrees from Technical University of Budapest, Hungary, in 1985 and 1991, respectively, in electrical engineering.

After graduation he joined the staff of the Department of Micrwave Telecommunication, Technical University of Budapest; first as a Research Fellow and then, beginning in 1987, as an Assistant Professor of Electrical Engineering. He has investigated wave propagation in inhomogeneous media, scattering from periodic and nonperiodic composite structures, and applied numerical methods for solution of scattering, antennas, and wave propagation problems. Since July 1990 to August 1992 he was a Visiting Research Associate at Syracuse University. He has investigated near-field to far-field transformation and numerical analysis of waveguides and printed circuits. He recently joined Compact Software Inc., Paterson, N.J. where he is a Senior Engineer of the Electromagnetic Group. His present fields of interest are numerical analysis of passive MIC and MMIC structures, and numerical methods in applied electromagnetics.

Dr. Petre has served as Cochairman of a Technical Session at the North American Radio Science Meeting and IEEE/AP-S Symposium, London, Ontario, 1991. He has authored and coauthored over 40 technical journal and conference papers.

Tapan K. Sarkar (S'69–M'76–SM'81–F'92) for a photograph and biography, see p. 234 of the February 1989 issue of this TRANSACTIONS.